Journal of Statistical Physics, Vol. 55, Nos. 3/4, 1989

Computer Simulation of Shock Waves in the Completely Asymmetric Simple Exclusion Process

C. Boldrighini,[1] G. Cosimi,[1] S. Frigio,[1] and M. Grasso Nuñes[2]

Received February 18; revision received July, 22, 1988

We study the evolution of the completely asymmetric simple exclusion process in one dimension, with particles moving only to the right, for initial configurations corresponding to average density ρ_- (ρ_+) left (right) of the origin, $\rho_- \leqslant \rho_+$. The microscopic shock position is identified by introducing a "second-class" particle. Results indicate that the shock profile is stable, and that the distribution as seen from the shock position $N(t)$ tends, as time increases, to a limiting distribution, which is locally close to an equilibrium distribution far from the shock. Moreover $N(t) \asymp V \cdot t$, with $V = 1 - \rho_- - \rho_+$, as predicted, and the dispersion of $N(t)$, $\sigma^2(t)$, behaves linearly, for not too small values of $\rho_+ - \rho_-$, i.e., $\sigma^2(t) \asymp S \cdot t$, where S is equal, up to a scaling factor, to the value S_{WA} predicted in the weakly asymmetric case. For $\rho_+ = \rho_-$ we find agreement with the conjecture $\sigma^2(t) \asymp \bar{S} \cdot t^{4/3}$.

KEY WORDS: Infinite-particle system; shock waves; asymmetric simple-exclusion process; zero-range process.

1. INTRODUCTION

The model study of microscopic situations that correspond to shock wave solutions of the Burgers equation is an important tool in investigating the phenomenon of persistence and propagation of shock waves. One would like to understand to what extent it makes sense to speak of shocks at the microscopic level. The natural questions are: what does the profile of a typical microscopic situation look like? to what extent can we speak of a microscopic shock position? and what is the microscopic state like in a neighborhood of that position?

For the simple exclusion model partial mathematical results have been obtained,[1-7] but they are far from giving us a satisfactory picture of

[1] Università degli Studi di Camerino, Camerino, Italy.
[2] ENEA Fellow, Permanent address: Via Bufalotta 5, 00139 Rome, Italy.
Dedicated to the memory of Paola Calderoni.

0022-4715/89/0500-0611$06.00/0

microscopic shock situations. A computer experiment was performed recently for a probabilistic cellular automaton which, like the simple exclusion model, contains an exclusion rule, and leads in the appropriate limit to the Burgers equation.[8] The results show that the microscopic configurations are in accordance, in the average, with the shock profile predicted by the Burgers equation. However, they do not allow conclusions on microscopic localization and persistence of the shock.

The purpose of the present work is to investigate by a computer experiment the localization and stability of microscopic shocks in the simple exclusion model. We consider only the completely asymmetric case: particles can jump only to the right. We find that by properly defining the miscroscopic shock position, as described below, the miscroscopic shock profile is stable in time.

To make the formulation of our results more clear, we first introduce the process. The one-dimensional simple exclusion (s.e.) process is described as follows. At each site of $\mathbb{Z}$ there is an exponential clock, i.e., a Poisson distributon of time with intensity 1. Clocks at different sites are independent. When the clock rings, the particle at that site chooses right or left with probabilities p and $1-p$, respectively, and jumps if the neighboring site is empty. If the neighboring site is occupied, nothing happens. We consider only the completely asymmetric case for which $p=1$. The one-dimensional s.e. process is a Markov process with state space $\mathbf{E}=\{0,1)^{\mathbb{Z}}$. The set of the extreme stationary translation-invariant measures is the set of the translation-invariant Bernoulli measures. For precise definitions and results the reader is referred to ref. 9.

Let us consider an initial configuration obtained by locating particles at the negative (positive) sites [i.e., left (right) of the origin] independently with probability ρ_- (ρ_+), i.e., a typical configuration of the product state $\mathbf{P}_{\rho_-}^{(-)}\times\mathbf{P}_{\rho_+}^{(+)}$, where $\mathbf{P}_{\rho_+}^{(+)}$ ($\mathbf{P}_{\rho_-}^{(-)}$) is a Bernoulli state with density ρ_- (ρ_+) on the negative (positive) sites. We take $\rho_-<\rho_+$ in order that the blocking effect which generates the shock may occur. At time 0 we have a shock, which is clearly visible if we take averages, since it corresponds to a jump $\rho_+-\rho_-$ in the occupation density at the site 0. Now the problem arises of keeping track of the microscopic shock position as time goes on. Suppose that we change the initial situation by locating at the negative empty sites "second-class particles" with density $(\rho_+-\rho_-)/(1-\rho_-)$, independently at each empty site. The dynamics of the second class (s.c.) particles is defined in such a way that they do not influence the motion of the previous, "first-class," particles: when the clock rings at a site occupied by a first-class particle, the particle jumps if the site at its right is either empty or occupied by a s.c. particle. In the second case the two particles exchange sites. When the clock rings at a site occupied by a s.c. particle, the particle jumps only

if the neighboring site is empty. Note that no s.c. particle can ever overcome a first-class one. Second-class particles have been introduced in studying the s.e. process as a technical device to describe a particular coupling of the process (see, for instance, ref. 3).

If we do not distinguish between first- and second-class particles, the evolution of our configuration is just the evolution of a typical equilibrium configuration corresponding to the density ρ_+. It is natural to think that the position of the first (rightmost) s.c. particle coincides with a discontinuity in the density of first-class particles, and hence can be identified with the shock position. To simplify computation, it is enough to add just one second-class particle at the origin at time 0 (to be called the s.c. particle). This we can do also when $\rho_+ = \rho_-$, though the procedure of adding extra particles with density $\rho_+ - \rho_-$ does not make sense. We speak of shock also in this case, though it is a somewhat different phenomenon.

Our way of locating the microscopic shock position turns out to work: the profile of the average occupation numbers around that position has a sharp break, which is stable in time. When speaking of shock position at time t we always intend the position at time t of the s.c. particle located at 0 at time 0, which is equal to the algebraic number of jumps $N(t)$ (i.e., number of forward jumps minus number of backward jumps) performed by the s.c. particle.

Since we follow the shock position, we are actually considering a different process, the process "as seen from the s.c. particle." When the s.c. particle jumps, we relable the sites in such a way that it is always at 0.

We report here results obtained for fixed $\rho_+ = 0.6$ and several values of $\rho_- \leqslant \rho_+$. Changing the parameters does not lead to qualitatively new results, provided that $\rho_- > 0$. Our results can be summarized as follows.

For all values of ρ_- the shock profile is stable around the shock position, and, moreover, computer results indicate that the local distribution of the occupation numbers at the sites close to the shock tends, as time grows, to a limiting distribution, which is the limiting distribution for the process as seen from the shock position. The distribution tends locally to the Bernoulli distribution with parameters ρ_+, ρ_- when we move away from the shock in the positive or negative directions. The falloff of the average occupation number profile to ρ_+, ρ_- as we move away from the shock is in agreement with predictions obtained by assuming some form of clustering for the limiting distribution. (Comparison with those predictions has been suggested to us by H. Spohn.) The falloff in the site position k should be exponential for $\rho_+ > \rho_-$, and power law $(1/k)$ for $\rho_+ = \rho_-$ (Section 2).

The drift velocity of the shock is known to be equal to

$1-\rho_+-\rho_-$,[10] and computer results are in very good agreement with this value. For the dispersion of the shock position $\sigma^2(t)$ computer results indicate that it behaves linearly in t in the range $0 \leqslant \rho_- < \beta$ for some $0.5 < \beta < 0.6$. Moreover, in this range the coefficient $S \equiv \lim_{t\to\infty}[\sigma^2(t)/t]$ turns out to be equal, within the error range, to

$$S_{\mathrm{WA}} = \frac{(1-\rho_+-\rho_-)(\rho_+ + \rho_-) + 2\rho_+\rho_-}{\rho_+ - \rho_-} \tag{1.1}$$

which, apart from a scaling factor, is the expression found for the weakly asymmetric simple exclusion process.[2]

For $\rho_+ = \rho_- = 0.6$ the growth of $\sigma^2(t)$ is faster and data are in agreement with the expected behavior $\sigma^2(t) = O(t^{4/3})$,[12] indicating the existence of long-range time correlations.

In the intermediate region $0.5 < \rho_- < 0.6$ computer results seem to indicate a growth of $\sigma^2(t)$ faster than t. The analysis of the transition region is, however, time-consuming and we are not able at present to draw definite conclusions.

2. COMPUTER SIMULATION

To perform computer simulations, it is convenient to use isomorphism of the simple exclusion process to the zero-range process (see, for instance, ref. 4 and references quoted there). The isomorphism is easily described in our case. The occupation number $\xi_k(t)$ of the zero-range process at site k and at time t is the number of empty sites between the kth particle (labeled from the origin) and the $(k+1)$th. When the kth particle jumps forward in the s.e. process, a zero-range particle jumps backward, i.e., $\xi_k \to \xi_k - 1$, $\xi_{k-1} \to \xi_{k-1} + 1$. When the second-class particle jumps backward (i.e., it exchanges places with a real one) ξ_0 takes the value of ξ_{-1}, which is zero, and all ξ_k take the value ξ_{k-1}, i.e., the whole configuration is shifted to the right.

We obtain an asymmetric zero-range process with state space $\mathbb{N}^{\mathbb{Z}}$.[9] The set of its extreme invariant measures is described as follows.[11] Occupation numbers at different sites are independent, and geometrically distributed with some parameter $\rho \in (0, 1)$, i.e., $\mathbf{P}(\xi_k = s) = \rho(1-\rho)^s$. This is the transform of the Bernoulli invariant measure of the simple exclusion process with parameter ρ.

We construct an initial zero-range configuration in the segment $[-L_1, L_2]$ in the following way. Occupation numbers are given independently at each site, according to a geometric distribution with parameter ρ_+ (ρ_-) in the segment $[0, L_2]$ ($[L_1, -1]$). We add a "source" at $L_2 + 1$ to

simulate incoming zero-range particles. The evolution is realized as follows. Let $\{\xi_j(T)\}_{j=-L_1}^{L_2}$ denote the occupation numbers at step T. At the next step $T+1$ the computer provides a realization k of a random variable with integer values, uniformly distributed in the range $[-L_1, L_2+1]$, and, if $k \in (-L_1, L_2]$ and $\xi_k(T) > 0$, performs the operations $\xi_k(T+1) = \xi_k(T) - 1$ and $\xi_{k-1}(T+1) = \xi_{k-1}(T) + 1$. If $k = -L_1$, the only change is $\xi_{-L_1}(T+1) = \xi_{-L_1}(T) - 1$ if $\xi_{-L_1}(T) > 0$. If $k = L_2 + 1$, then with probability ρ_+ nothing happens and with probability $1-\rho_+$, $\xi_{L_2}(T+1) = \xi_{L_2}(T) + 1$. All other occupation numbers are unchanged. If $k = -1$ and $\xi_{-1}(T) = 0$, then $\xi_k(T+1) = \xi_{k-1}(T)$, $k \in (-L_1, L_2]$, and ξ_{-L_1} is generated as for the initial configuration.

Our time variable t is given by the number of steps divided by $L_1 + L_2 + 2$: $t = T/(L_1 + L_2 + 2)$. Before taking any measure we always let the system evolve for a time $t_0 = 100{,}000$, in order to make sure that we are close to the stationary limiting distribution.

For all results reported in this paper $L_1 = L_2 = L$. The influence of the finite length is estimated by comparing results for different values of L. Typically, L is considered large enough when by doubling it the result changes by less than 1%. The same empirical rule has been sometimes used for the length of time intervals over which averages are taken. The values of L and the averaging time are always indicated in the figure captions.

One should also discuss the influence of the mechanism which generates the random numbers. A detailed discussion of this point is, however, out of place in this paper. We assume throughout that the random number generation is "perfect." As a check, one can look at the behavior of the fluctuations of the averages $N(t)/t$ around the expected value, which should fall off as $1/\sqrt{t}$ for parameter values for which the central limit theorem is expected to hold. For $\rho_- = 0.2$, $\rho_+ = 0.6$ the behavior is shown in Fig. 4 (Section 4).

The basic quantities we compute are the following. (*i*) The joint probability distributions of s sites $k_1, \ldots, k_s$, $\mathbf{P}_{k_1,\ldots,k_s}(j_1,\ldots,j_s) \equiv \mathbf{P}(\xi_{k_1} = j_1, \ldots, \xi_{k_s} = j_s)$, which are computed by taking time averages of the corresponding characteristic functions. (ii) $N(t)$, the algebraic number of jumps of the second-class particle in the simple exclusion process up to time t. This is computed in terms of the zero-range process as follows: when the occupation number of ξ_0 decreases by one, we add $+1$, and when the configuration is shifted to the right, we add -1.

Reconstruction of probabilities for the s.e. process from the computed quantities $\mathbf{P}_{k_1,\ldots,k_s}(j_1,\ldots,j_s)$ is made by using the inverse transformation. This does not introduce further errors since any occupation probability for the s.e. process involves only a finite sum over the zero-range probabilities $\mathbf{P}_{k_1,\ldots,k_s}(j_1,\ldots,j_s)$.

Data were taken using a Microvax computer at the Centro di Calcolo of the University of Camerino and the CRAY X-MP/12 of CINECA, Bologna.

3. SHOCK STRUCTURE AND LIMITING DISTRIBUTION

We denote by $\eta_k \in \{0, 1\}$ the value of the s.e. process at site k (counted from the shock position). The computer results for the asymptotic average occupation numbers $\mathbf{E}\eta_k$ are shown in Fig. 1 for $\rho_+ = 0.6$, $\rho_- = 0.4$, and $\rho_+ = \rho_- = 0.6$, in the range $-40 < k < 40$.

It is useful to compare the results shown in Fig. 1 with theoretical predictions obtained under obvious clustering and stationarity assumptions. In the stationary regime the average number of particles in the interval $(0, L]$ is constant, so the average incoming and outcoming flows are equal. L should be considered very large, i.e., we are actually taking the limit $L \to \infty$, so that we can assume that the local distribution near L is given by the equilibrium measure with parameter ρ_+, and is independent of η_1, η_{-1}. It is readily seen that the rate at which particles enter in the interval at 0 is $\mathbf{E}\eta_{-1}$, and the net rate at which particles get out of it at L is $\rho_+ \mathbf{E}\eta_{-1} + \rho_+(1-\rho_+) - \rho_+(1-\mathbf{E}\eta_1)$, so that we get the equation

$$\rho_+ \mathbf{E}\eta_{-1} + \rho_+(1-\rho_+) = \rho_+(1-\mathbf{E}\eta_1) + \mathbf{E}\eta_{-1} \tag{3.1a}$$

The balance in the interval $[-L, 0)$ gives, similarly,

$$\rho_- \mathbf{E}\eta_{-1} + \rho_-(1-\rho_-) = \rho_-(1-\mathbf{E}\eta_1) + \mathbf{E}\eta_{-1} \tag{3.1b}$$

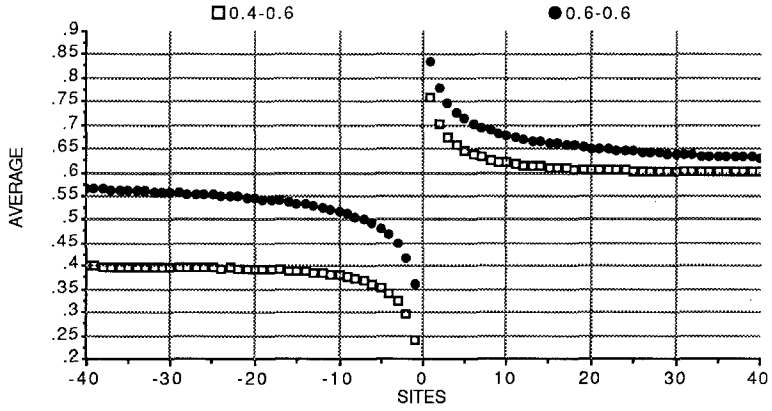

Fig. 1. Average occupation numbers for the s.e. process as seen from the shock position. Averaging time $3 \cdot 10^6$. Here $L = 60$.

Solving for the forward and backward jump rates $a = 1 - \mathbf{E}\eta_1$ and $b = \mathbf{E}\eta_{-1}$, we get $a = 1 + \rho_+\rho_- - \rho_+ - \rho_-$, $b = \rho_+\rho_-$, or

$$\mathbf{E}\eta_1 = \rho_+ + \rho_-(1-\rho_+)$$

$$\mathbf{E}\eta_{-1} = \rho_- - \rho_-(1-\rho_+)$$

which is in very good agreement with the results shown in Fig. 1.

The difference of the forward and the backward jump rates gives the drift, i.e., the asymptotics of the average value $\mathbf{E}N(t)/t$ for $t \to \infty$, which is $a - b = 1 - \rho_+ - \rho_- = V(\rho_-, \rho_+)$, as it should be.[10]

When we move away from the shock position the local distribution should tend to the equilibrium one, and, in particular, occupation numbers at different sites should become independent. Figure 2 shows the variation distance between the computed joint distribution for two neighboring sites, k, $k+1$ for $k > 1$, and $k-1$, k, for $k \leqslant -1$, and the product of binomial distributions with the computed parameters $\mathbf{E}\eta_k$, $\mathbf{E}\eta_{k+1}$ ($\mathbf{E}\eta_{k-1}$, $\mathbf{E}\eta_k$), as a function of k. We recall that the variation distance between the joint distributions $\mathbf{P}_1$, $\mathbf{P}_2$ of two random variables taking values 0, 1 is given by

$$\mathrm{Var}(\mathbf{P}_1, \mathbf{P}_2) \equiv \frac{1}{2} \sum_{j_1=0}^{1} \sum_{j_2=0}^{1} |\mathbf{P}_1(j_1, j_2) - \mathbf{P}_2(j_1, j_2)|$$

The results show that approximate independence holds already fairly close to the shock position, and it is established earlier for $\rho_+ = 0.6$, $\rho_- = 0.4$ than for equal densities $\rho_+ = \rho_- = 0.6$.

Assuming that the two-site joint distribution approximately factorizes already for values of k for which the average $\rho_k = \mathbf{E}\eta_k$ is still significantly

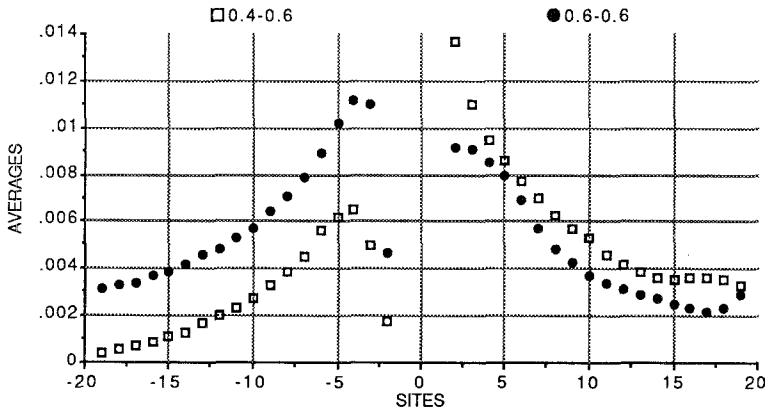

Fig. 2. Variation distance between joint distribution and product distribution for neighboring sites for $\rho_+ = 0.6$ and $\rho_- = 0.4$, 0.6. Averaging time $3 \cdot 10^6$. Here $L = 60$.

different from the asymptotic values ρ_+, ρ_-, the decay of the asymptotic profile can be predicted using again balance arguments. Equating incoming and outcoming rates for the interval $[k, L)$, $k>0$, where again we take $L\to\infty$, we get, in analogy with Eq. (3.1a),

$$\rho_k b+\rho_+ a+\rho_k(1-\rho_{k+1})=\rho_{k+1}b+\rho_+(1-\rho_+)+a\rho_+$$

so that, setting $\delta_k=\rho_k-\rho_+$, we get the recursion relation $(a+\rho_k)\,\delta_{k+1}=(b+1-\rho_+)\,\delta_k$. If $\rho_-<\rho_+$, we can neglect δ_k with respect to ρ_+ for large k and we get $\delta_{k+1}=a\delta_k$ with $a=(1+\rho_+\rho_--\rho_+)/(1+\rho_+\rho_--\rho_-)$, i.e., δ_k falls off exponentially, $\delta_k\asymp a^k$. If $\rho_-=\rho_+=\rho$, we find instead

$$\delta_{k+1}=\frac{c}{c+\delta_k}\,\delta_k$$

where $c=1+\rho^2-\rho$. Setting $\delta_k=c(S_k+1)/k$, we find the recursion relation $S_{k+1}=S_k/(1+1/k)$ which implies $S_k\to 0$ for $k\to\infty$, i.e., asymptotically $\delta_k\asymp c/k$.

For $\rho_-=0.4$, $\rho_+=0.6$ the data show definitely exponential decay rather then power law; the slope of $\log\delta_k$ versus k in the range $5\leqslant k\leqslant 32$, computed by a linear best fit, is -0.115, indicating a behavior of the type α^k with $\alpha=0.89$, to be compared to the predicted value $\alpha=0.76$. For better agreement one should presumably take larger values of k.

For $\rho_+=\rho_-=0.6$ the decay of δ_k as k grows is slower, as shown by Fig 1. A linear best fit of δ_k versus $1/k$ in the range $15\leqslant k\leqslant 35$, shown in Fig. 3, indicates excellent agreement with the predicted c/k behavior. The computed slope turns out to be 0.755, very close to the predicted value 0.76.

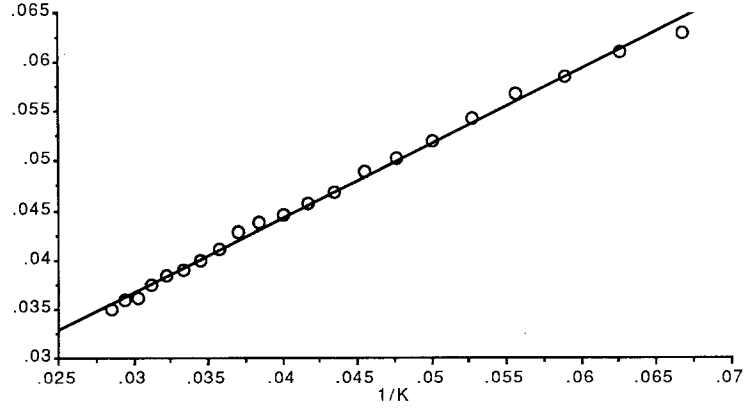

Fig. 3. Plot of δ_k versus $1/k$. Averaging time $3\cdot 10^6$. Here $L=60$.

4. DRIFT VELOCITY AND DISPERSION. COMPARISON WITH THEORETICAL RESULTS

As mentioned above, the drift velocity of the shock wave is known to be equal to $V(\rho_-, \rho_+) = 1 - \rho_+ - \rho_-$. Numerically this is computed by taking the average $N(t)/t$. The dispersion of the jump number is more difficult to compute, since one should take ensemble averages over different initial conditions distributed according to the stationary distribution. We have discarded such a procedure, since it would consume too much computer time. Instead, we estimate the dispersion of the jump number $\sigma^2(\tau) = \mathbf{E}(N(\tau) - V \cdot \tau)^2$ by the ergodic average

$$\sigma^2(M; \tau) = \frac{1}{M} \sum_{k=0}^{M-1} \left[N(k\tau, (k+1)\tau) - \frac{N(M \cdot \tau)}{M} \right]^2 \tag{4.1}$$

where $N(t_1, t_2)$ is the number of jumps in the time interval (t_1, t_2). We are actually interested in the behavior of $\sigma^2(\tau)$ for large τ. A linear behavior in τ: $\sigma^2(\tau) \asymp S(\rho_+, \rho_-)\,\tau$ indicates strong decay of time correlations for the process $N(t)$, and hence validity of the CLT for $(1/\sqrt{\tau})\,\hat{N}(\tau)$ $[\hat{N}(\tau) \equiv N(\tau) - V \cdot \tau]$. To estimate how far $\sigma^2(M; \tau)$ is from its average value $\sigma^2(\tau)$, observe that the difference can be written as

$$\Delta\sigma^2(M; \tau) \equiv \sigma^2(M; \tau) - \sigma^2(\tau) = \frac{1}{M} \sum_{k=0}^{M-1} (\hat{N}_k)^2 - \mathbf{E}(\hat{N}_k)^2 \tag{4.2}$$

where

$$\tilde{N}_k \equiv N(k\tau, (k+1)\tau) - \frac{N(M \cdot \tau)}{M}, \qquad \hat{N}_k \equiv N(k\tau, (k+1)\tau) - V \cdot \tau$$

By adding and subtracting $(\hat{N}_k)^2$, we get

$$\Delta\sigma^2(M; \tau) = \frac{1}{M} \sum_{k=0}^{M-1} \{[(\tilde{N}_k)^2 - \mathbf{E}(\hat{N}_k)^2]\} - \left[\frac{N(M \cdot \tau)}{M} - V \cdot \tau \right]^2 \tag{4.3}$$

If there is fast decay of correlations, the last term on the rhs of Eq. (4.3) is $O(\tau/M)$ and is negligible with respect to the first one, since for large τ

$$\begin{aligned} S_M^2(\tau) &\equiv M\mathbf{E} \frac{1}{M} \sum_{k=1}^{M-1} \{[(\hat{N}_k)^2 - \mathbf{E}(\hat{N}_k)^2]\}^2 \\ &= [\mathbf{E}\hat{N}_0^4 - (\mathbf{E}\hat{N}_0^2)^2][1 + O(1)] = O(\tau^2) \end{aligned} \tag{4.4}$$

By Eq. (4.4), $S_M^2(\tau)$ can be estimated by the ergodic average

$$S^2(M; \tau) = \frac{1}{M} \sum_{k=0}^{M-1} [\hat{N}_k^2 - \sigma^2(M; \tau)]^2$$

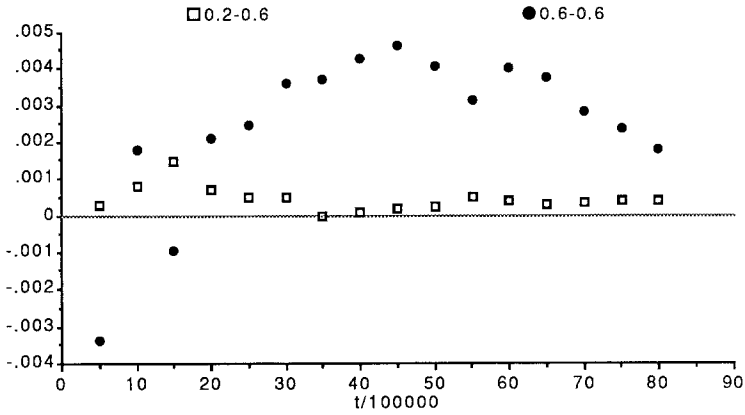

Fig. 4. Behavior of $N(t)/t - V(\rho_-, \rho_+)$. Averaging time $8 \cdot 10^6$. Here $L = 120$.

and we have

$$\mathbf{E}(\Delta\sigma^2(M;\tau))^2 \approx \frac{1}{M} S^2(M;\tau) \tag{4.5}$$

Figure 4 shows the behavior of $N(t)/t - V(\rho_-, \rho_+)$ versus t for $\rho_- = 0.2$, $\rho_+ = 0.6$, and $\rho_- = \rho_+ = 0.6$. It is apparent that the variance for $\rho_+ = \rho_- = 0.6$ is much larger, in agreement with the behavior for the dispersion of $N(t)$, $\sigma^2(t) \asymp \bar{S} \cdot t^{4/3}$, which is discussed below [for $\rho_- = 0.2$, $\rho_+ = 0.6$, we find $\sigma^2(t) \asymp S_{\mathrm{WA}} \cdot t$]. All data in Fig. 3 are in absolute value less then $2\sigma(t)/t$, i.e., within two standard deviations.

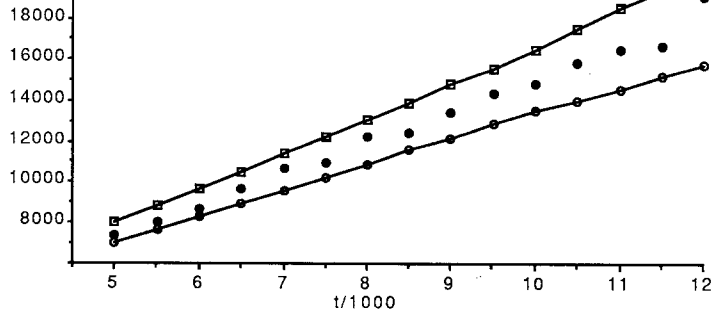

Fig. 5. Behavior of $\sigma^2(M;t)$, where $M \cdot t = 8 \cdot 10^6$, $\rho_- = 0.3$, $\rho_+ = 0.6$, $L = 120$. Upper and lower curves correspond to $S_{\mathrm{WA}} \cdot t \pm 2[S^2(M;t)/M]^{1/2}$.

We have computed $S_M^2(t)$ and $\sigma^2(M; t)$ for $\rho_- = 0.1$, 0.2, 0.3, 0.4, 0.5, 0.55, 0.6. We have taken $L = 120$, since in the upper range of ρ_- the results seem to be sensitive to the configuration length for lower values of L, in the chosen range of t: $5000 \leqslant t \leqslant 12{,}000$. (This is further discussed at the end of the section.) The t range has been determined by the requirement that t should be large enough to be in the asymptotic region for all values of ρ_-. For $\rho_- < 0.5$ the asymptotic regime is actually reached for much smaller values of t.

Figure 5 shows the behavior of $\sigma^2(M; t)$ for $\rho_- = 0.3$ as a function of t. Data for different t correspond to different M, as $M \cdot t$ is held constant, so that we could get estimates of $\sigma^2(t)$ for different values of t in the same run.

Figure 5 shows that results are consistent with the prediction $\sigma^2(t) \asymp S \cdot t$ with $S = S_{\mathrm{WA}}$, where S_{WA} is the weakly asymmetric prediction given by Eq. (1.2). We have checked that the same holds for $\rho_- = 0.1$, 0.2, 0.4, and 0.5.

For $\rho_- = 0.6$ we should have long-time correlations,[12] and relation (4.4) cannot be expected to hold any more. The best straight line approximating our data in a $\ln \sigma^2(M; t)$ versus $\ln t$ plot has a coefficient which differs from 4/3 by less than 1%. One can estimate $\bar{S}$ as the coefficient of the best linear function in $t^{4/3}$ which approximates our data $\sigma^2(M; t)$, giving $\bar{S} = 0.67$ (with a 1% rounding off). The coefficient should be compared with the approximate theoretical prediction of ref. 12, which is $\approx 1.86[\rho(1-\rho)]^{2/3}$, or ≈ 0.7.

Though the theoretical significance of the bounds is doubtful, Fig. 6 shows accordance with the $\sigma^2(t) \asymp \bar{S} \cdot t^{4/3}$ prediction.

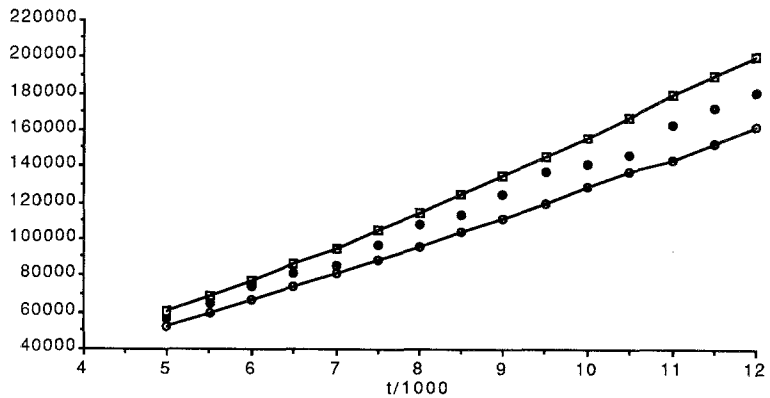

Fig. 6. Behavior of $\sigma^2(M; t)$, where $M \cdot t = 8 \cdot 10^6$, $\rho_- = 0.6$, $\rho_+ = 0.6$, $L = 120$. Upper and lower curves correspond to $S \cdot t \pm 2[S^2(M; t)/M]^{1/2}$.

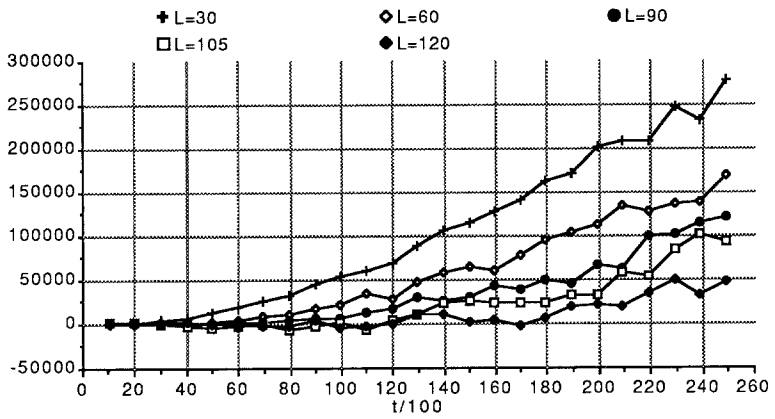

Fig. 7. Behavior of the difference between $\bar{S} \cdot t^{4/3}$ and the computed dispersion.

A few more words should be said about the choice of the interval length and of the averaging time. Clearly, time should be large enough to pick up the asymptotic behavior of the dispersion. But if it is too long, then the extra random effects coming from the border begin to be felt, and eventually lead to a linear behavior in t for the dispersion. This effect is shown in Fig. 7, where the behavior of the difference between $\bar{S} \cdot t^{4/3}$ and the computed dispersion is shown for five different values of the interval length.

ACKNOWLEDGMENTS

We thank Errico Presutti for stimulating our interest in the problem and Anna De Masi and Herbert Spohn for valuable suggestions and discussions. The work of C.B., G.C., and S.F. was supported in part by CNR PS-AITM and MPI.

REFERENCES

1. H. Rost, Non-equilibrium behaviour of a many particle process: Density profile and local equilibria, *Z. Wahrsch. Verw. Geb.* **58**:41–53 (1981).
2. A. De Masi, E. Presutti, and E. Scacciatelli, The weakly asymmetric simple exclusion process, CARR Reports No. 4 (1987).
3. E. D. Andjel, M. D. Bramson, and T. M. Liggett, Shock in the asymmetric simple exclusion, Preprint (1987).
4. P. A. Ferrari, The simple exclusion process as seen from a tagged particle, *Ann. Prob.* **14**:1277–1290 (1986).

5. A. De Masi, C. Kipnis, E. Presutti, and E. Saada, Microscopic structure at the shock in the asymmetric simple exclusion, Preprint (1986).
6. C. Kipnis, Central limit theorems for infinite series of queues and applications to simple exclusion, *Ann. Prob.* **14**:397–408 (1986).
7. W. D. Wick, A dynamical phase transition in an infinite particle system, *J. Stat. Phys.* **38**:1015–1025 (1985).
8. B. M. Boghosian and C. D. Levermore, A cellular automaton for Burger's equation, *Complex Syst.* **1**:17–30 (1987).
9. T. M. Ligget, *Interacting Particle System* (Springer, New York, 1985).
10. E. D. Andjel and M. E. Vares, Hydrodynamic equations for attractive particle systems on $\mathbb{Z}$, *J. Stat. Phys.* **47**:265–288 (1987).
11. E. Andjel, Invariant measures for the zero range process, *Ann. Prob.* **10**:525–547 (1982).
12. H. van Beijeren, R. Kutner, and H. Spohn, Excess noise for driven diffusive systems, *Phys. Rev. Lett.* **18**:2026–2029 (1985).